Vol. 75: 143–154, 2018
https://doi.org/10.3354/cr01514

CLIMATE RESEARCH
Clim Res

Published online May 30

Recent aridity trends and future projections in the Nemunas River basin

Edvinas Stonevičius[1], E. Rimkus[1], J. Kažys[1,*], A. Bukantis[1], J. Kriaučiūnienė[2], V. Akstinas[2], D. Jakimavičius[2], A. Povilaitis[3], L. Ložys[4], V. Kesminas[4], T. Virbickas[4], V. Pliūraitė[4]

[1]Institute of Geosciences, Vilnius University, 03101 Vilnius, Lithuania
[2]Lithuanian Energy Institute, 44403 Kaunas, Lithuania
[3]Aleksandras Stulginskis University, 53361 Kaunas-Akademija, Lithuania
[4]Nature Research Centre, 08412 Vilnius, Lithuania

ABSTRACT: Changes in the reference evapotranspiration (ET_0) and precipitation (*P*) patterns in the Nemunas River basin (Baltic Sea catchment) are evident today and will be even more significant in the future. Nemunas basin aridity dynamics (1901–2010) and projections (2081–2100) were evaluated using the UNEP aridity index (AI). Historical analysis (CRU TS3.24.01) and future projections (EURO-CORDEX) of monthly air temperature and precipitation were used for the AI estimation. Projections of the meteorological parameters according to 4 Representative Concentration Pathway scenarios (RCP2.6, 4.5, 6.0 and 8.5) were used in the analysis. In the Nemunas River basin, evapotranspiration exceeded precipitation from April to August, and in a large part of the basin the climatic conditions during this part of the year could be described as dry subhumid (AI < 0.65). Since the 1980s, increased aridity has been observed between April and August due to a strong positive trend of ET_0 and a strong negative trend of *P*. Future projections (2081–2100) show that despite large uncertainties in the climate projections, it is more likely that the Nemunas basin climate will become more humid in April and May and drier between June and August. The increase in climate aridity during these months is more likely in the southern and central parts of the basin.

KEY WORDS: Nemunas basin · Reference evapotranspiration · Precipitation · Aridity index · AI · EURO-CORDEX · Climate change

1. INTRODUCTION

Due to climate change, increased aridity is a growing problem in many parts of the world (Paltineanu et al. 2007, Zhang et al. 2009, Tabari & Aghajanloo 2013). These tendencies are the most critical for residents of the subtropical climate zone (Huo et al. 2013, Tabari & Aghajanloo 2013), although this issue will also become more important in mid-latitudes. Until now, changes in aridity in the latter region have been poorly investigated. According to IPCC (2013), the air temperature will increase with varying magnitudes during the 21st century over land territories, while changes in the amount of precipitation will be uneven across the planet. In some places (e.g. the Nemunas River basin) an air temperature rise will be followed by a negligible increase in precipitation, so it is very important to understand how climate change will impact the aridity in these areas.

There are many methods for determining the state of aridity/humidity in particular catchments (Maliva & Missimer 2012). The ratio between precipitation and air temperature that was used for the very first indices was proposed by De Martonne (1926) and

*Corresponding author: justas.kazys@gf.vu.lt

Selianinov (1928). For evaluation of river catchment conditions, evapotranspiration is used instead of temperature (Thornthwaite 1948, Palmer 1965, UNESCO 1979). It is possible to calculate evapotranspiration using different methods (Penman 1948, Budyko 1958, Hargreaves 1994). Drought indices based on precipitation (McKee et al. 1993) and fluctuations in river runoff (Nalbantis & Tsakiris 2009) could also be indicators of change in aridity in the catchment area (Rimkus et al. 2013). The Köppen-Geiger climate classification (Rubel & Kottek 2010) and Worldwide Bioclimatic Classification System (Rivas-Martinez et al. 2011) also illustrate catchment water availability patterns in an indirect way.

The UNEP aridity index (AI; abbreviations in Table 1) is based on the ratio between precipitation (*P*) and potential evapotranspiration (PET) (UNESCO 1979). Alteration of the AI index due to the impacts of climate change has been reported worldwide (Sailer 2013, Girvetz & Zganjar 2014) and for different catchments (Arora 2002, Paulo et al. 2012, Ficklin et al. 2013, Fniguire et al. 2014, Li & Chen 2015). In particular, aridity trends have a regional basis, e.g. an increase in aridity was demonstrated in most of southern Europe (Paltineanu et al. 2007, Colantoni et al. 2015), while no annual trends were observed in Serbia (Hrnjak et al. 2014). In the northern part of the US Great Plains aridity decreased, while in the southern part it increased (Kukal & Irmak 2016).

Climate change is already having a great impact on river water regimes. In rivers supplied by snowmelt, atmospheric temperature increases not only affect freshwater ecosystems via the warming of the water, but also by causing water-flow alterations (Kundzewicz et al. 2007). The projected impacts on a basin depend on the sensitivity of the catchment to changes in climatic characteristics and on the projected changes in the magnitude and seasonal distribution of precipitation, temperature and evaporation (Jiménez Cisneros et al. 2014). The detected trends in river runoff have generally been consistent with observed regional changes in precipitation and temperature since the 1950s. In Europe, river runoff (1962–2004) has decreased in the south and east and generally increased in the north (Wilson et al. 2010, Stahl et al. 2012).

Out of all the ecosystems, freshwater ecosystems have the highest proportion of species threatened with extinction due to climate change (Millennium Ecosystem Assessment 2005). The streamflow-mediated ecological impacts of climate change are expected to be stronger than the historical impacts due to anthropogenic alterations of flow regimes by water withdrawal and the construction of reservoirs (Jiménez Cisneros et al. 2014). Changes in climate and land use will put additional pressures on already stressed riparian ecosystems along many rivers in the world (Naiman et al. 2005).

This article analyses the territory (52.0–56.5° N, 21.0–28.5° E) which covers the Nemunas River basin (hereafter Nemunas basin) (Fig. 1). The Nemunas River is in the eastern part of the Baltic Sea catchment (Fig. 1). It is the 14th longest European river (937 km) and flows through Belarusian, Lithuanian and Russian Federation (Kaliningrad district) territories. These 3 countries cover 97.3% of the total basin area (98 200 km^2). Only the upper reaches of the some tributaries are located in Poland and Latvia.

The average annual temperature (1981–2010) in the Nemunas basin is 6.8°C. The average air temperature during winter is –2 to –6°C, while in the summer it goes up to 16–18°C. Permanent snow cover usually forms by mid-December and disappears by the middle of March. The average amount of annual precipitation in the basin's territory is 672 mm. In general, most of the precipitation falls in summer.

On average, annual river discharge is 21 km^3. From this amount, 41–46% of the water flows in spring, 15–18% in summer, 19–22% in autumn and 17–21% in winter. The maximum discharge in spring is due to flooding caused by snowmelt.

In the Baltic Sea catchment aquatic ecosystem, most ecologically important factors are affected by climate change (BACC Author Team 2008). No significant long-term change in river runoff over the last 500 yr has been detected in the Baltic catchment

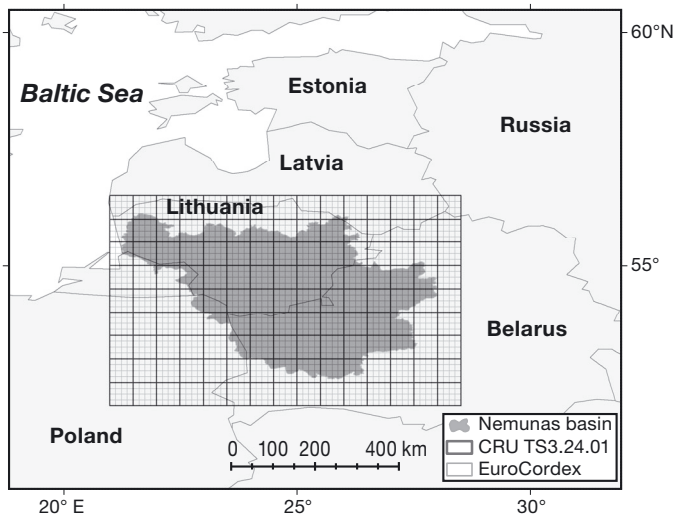

Fig. 1. Nemunas River basin and database grids used for the historical analysis of aridity (CRU TS3.24.01) and future projections (CMIP 5)

Table 1. Abbreviations used in the study

Abbreviation	Explanation
P	Precipitation
PET	Potential evapotranspiration: the amount of evaporation that would occur if a sufficient water source were available.
ET_0	Reference evapotranspiration: evapotranspiration from the reference surface, which is a hypothetical grass reference crop with an assumed crop height of 0.12 m, a fixed surface resistance of 70 s m^{-1} and an albedo of 0.23
AI	UNEP aridity index
GCM	General circulation models
CMIP5	Coupled Model Intercomparison Project Phase 5
RCP	Representative concentration pathways
RCM	Regional climate model
CORDEX	Coordinated Regional Climate Downscaling Experiment
EURO-CORDEX	European branch of the CORDEX initiative
RCA4	Rossby Centre regional climate model
MOHC-HadGEM2-ES	UK Met Office Hadley Global Environment Model 2 - Earth System
MPI-M-MPI-ESM-LR	Earth system model of the Max-Planck-Institut für Meteorologie - low resolution
ICHEC-EC-EARTH	The Irish Centre for High-End Computing EC-EARTH earth system models

(BACC II Author Team 2015); however, alterations of river runoff regimes, especially seasonal patterns of flow, are evident in the eastern part of the basin (Klavins et al. 2002, Kriauciuniene et al. 2012, Sarauskiene et al. 2015). The Nemunas basin has also experienced a shift (since the 1960s) from a natural hydrological cycle (Jablonskis 1992, Volchak 2004, Meilutytė-Barauskienė et al. 2008) to anthropogenically induced regime changes (Kriaučiūnienė et al. 2008, Rimkus et al. 2013, Stonevičius et al. 2014). In the future, changes to climatic conditions will be important for Nemunas basin hydrology (Kilkus et al. 2006, Kriaučiūnienė et al. 2008, Stonevičius et al. 2017).

The main objective of this research was to analyse aridity changes in the Nemunas basin, assessing the influence of reference evapotranspiration (ET_0) and *P* on aridity. The P:ET_0 ratio perfectly illustrates river basin inter- and intra-annual water availability fluctuations, especially during the vegetation period (April–August). For this purpose, we evaluated aridity dynamics (1901–2010) and future projections of climate aridity (2081–2100). The results will help to evaluate the Nemunas basin's water balance, river runoff change and possible climate change impacts on the ecological and socio-economic state of the basin with regard to the EU Water Framework Directive (ter Heerdt et al. 2007). Moreover, it is a solid background for the development of international collaboration projects tackling climate change challenges in transboundary rivers, which have already started (Korneev et al. 2015).

2. MATERIALS AND METHODS

The CRU TS3.24 monthly high-resolution (0.5 × 0.5°) grid time series, which were developed by the University of East Anglia Climatic Research Unit, were used for analysing the AI change in the research area from 1901–2010 (Harris & Jones 2017). Climate projections for the 21st century were based on General Circulation Model (GCM) outputs, which are part of the Coupled Model Intercomparison Project Phase 5 (CMIP5) (Taylor et al. 2012). However, GCMs only provide general conditions; for medium-sized areas such as the Nemunas basin, the outputs of Regional Climate Models (RCM) should be used. We chose the EURO-CORDEX (www.euro-cordex.net) initiative data sets. EURO-CORDEX is the European branch of the CORDEX initiative, and produces ensemble climate simulations based on multiple dynamic and empirical–statistical downscaling models forced by multiple global climate models from CMIP5.

The CORDEX RCM simulations for the European domain (EURO-CORDEX) are conducted at 2 different spatial resolutions: a general CORDEX resolution of 0.44° (EUR-44; ~50 km), and a finer resolution of 0.11° (EUR-11; ~12.5 km). The ensemble consists of 17 simulations carried out by 7 different models at grid resolutions of 12 km (9 experiments) and 50 km (8 experiments) (Kotlarski et al. 2014). The first EUR-11 simulations were published and distributed via the Earth System Grid Federation (ESGF) and were available from 2013. The DKRZ ESGF-CoG Node (https://esgf-data.dkrz.de/search/cordex-dkrz/) was used for downloading the data.

For our research purposes, the RCM data had to meet the following requirements — experiments: his-

torical, RCP2.6, RCP4.5, RCP8.5; research area: Nemunas River basin; time frequency: monthly values; variable: precipitation, maximum, mean and minimum air temperatures near the surface. Only the RCA4 simulations met all the requirements.

The coupled atmosphere–ice–ocean model RCA4-NEMO (Dieterich et al. 2013, Wang et al. 2015) was developed by the Rossby Centre at the Swedish Meteorological and Hydrological Institute (SMHI) for regional climate simulations and the regionalization of climate change scenarios. RCA4 has been used for different domains in the CORDEX project, including Europe (Wang et al. 2015). The model's domain of applicability is northern Europe. The spatial resolution of the model for the atmosphere is 0.22° and 40 vertical levels. It consists of the RCA4 atmosphere model in a model domain covering the eastern Atlantic and Europe (Kupiainen et al. 2014) and the ocean model NEMO setup for the North Sea and Baltic Sea (Hordoir et al. 2013). The Rossby Centre has produced and made available a huge number of CORDEX simulations. The data set is unique because RCA4 takes lateral boundary conditions from a very large number of different GCMs (Strandberg et al. 2014). In this research, we used the historical, RCP2.6, RCP4.5 and RCP8.5 simulations for the CMIP5 scenarios using the GCMs MOHC-HadGEM2-ES (Collins et al. 2011), MPI-M-MPI-ESM-LR (Giorgetta et al. 2013) and ICHEC-EC-EARTH (Hazeleger et al. 2010) boundary conditions.

The aridity of the investigated territory was determined by calculating the AI (Middleton & Thomas 1997):

$$\mathrm{AI} = \frac{P}{\mathrm{ET}_0} \tag{1}$$

In this study, AI was calculated using ET_0 instead of potential evapotranspiration used in MAB technical notes 7 (UNESCO 1979). Potential evaporation defines the amount of evaporation that would occur if a sufficient water source were available, while ET_0 is defined more specifically: ET_0 is evapotranspiration from a reference surface, which is a hypothetical grass reference crop with an assumed crop height of 0.12 m, a fixed surface resistance of 70 m s^{-1} and an albedo of 0.23 (Allen et al. 1998).

The original Hargreaves equation (Hargreaves 1994) was used to calculate the monthly averaged ET_0:

$$\mathrm{ET}_0 = C\ R_a\,(T_{\max} - T_{\min})^{0.5}\,(T + 17.8) \tag{2}$$

where C is a coefficient whose value is 0.0023 (Hargreaves & Samani 1985), R_a is the water equivalent of the monthly averaged daily extraterrestrial radiation (mm d^{-1}), and $T_{\max}$, $T_{\min}$ and T are the monthly averaged maximum, minimum and mean air temperatures. R_a is calculated from the latitude and month of the year.

In this study the average annual and monthly values of the analysed parameters were calculated for the period from 1981–2010 (Fig. 2). P and ET_0 had a similar annual pattern in the Nemunas basin; both parameters had higher values during the warm season than during the cold season. The rate of change of ET_0 in spring and autumn was higher than P, thus from April to August ET_0 exceeded P. Changes in the P and ET_0 during these months might lead to the most significant effect on the hydrology and ecology of the Nemunas basin. According to Middleton & Thomas (1997), an AI value <0.65 can be considered an indicator of dry conditions. This study only analysed the dry period (the AI during this time of year was <0.65) lasting from April to August (Fig. 2).

The linear trend values of P, ET_0 and AI for each grid cell were calculated using the non-parametric Sen's slope method (Helsel & Hirsch 1992). Statistical significance ($\alpha < 0.05$) of the trends was evaluated using a non-parametric Mann-Kendall test.

Air temperature (maximum, mean and minimum) and precipitation amount projections for 21st century were used to create AI forecasts. The projected changes were calculated as the air temperature difference (°C) or precipitation amount ratio (%) between different periods of the 21st century and the reference period (1986–2005) in every grid cell. The long-term changes were evaluated by comparing the averages of the meteorological variables between two 20 yr periods (1986–2005 and 2081–2100).

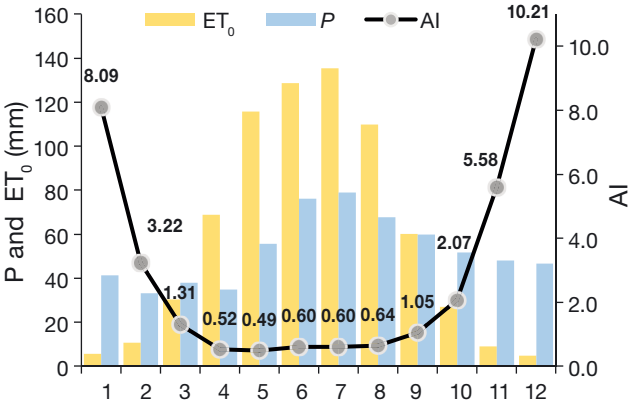

Fig. 2. Mean annual pattern of reference evapotranspiration (ET_0), precipitation (P) and aridity index (AI) in the Nemunas basin in 1981–2010

3. RESULTS

3.1 Aridity dynamics during 1901–2010

During the dry period (April–August), the highest ET_0 and P values were recorded in the southeastern part of the region in July (Fig. 3). Due to the cooling effect of the Baltic Sea, the lowest ET_0 values were recorded in the coastal zone in every month of the dry period. Meanwhile, the precipitation patterns gradually changed. At the beginning of the season more precipitation fell in the eastern part of this region, while in August the rainfall peak moved to the northwest. The highest AI values were observed in this area in August. During the remaining months the AI values were below 0.8 for the whole territory, and in a large part of the region the climatic conditions could be considered dry subhumid (<0.65). Due to the low amount of precipitation, the lowest AI values were recorded between April–June.

The mean annual ET_0 was higher than the mean annual P by an average of 62 mm during 1901–2010

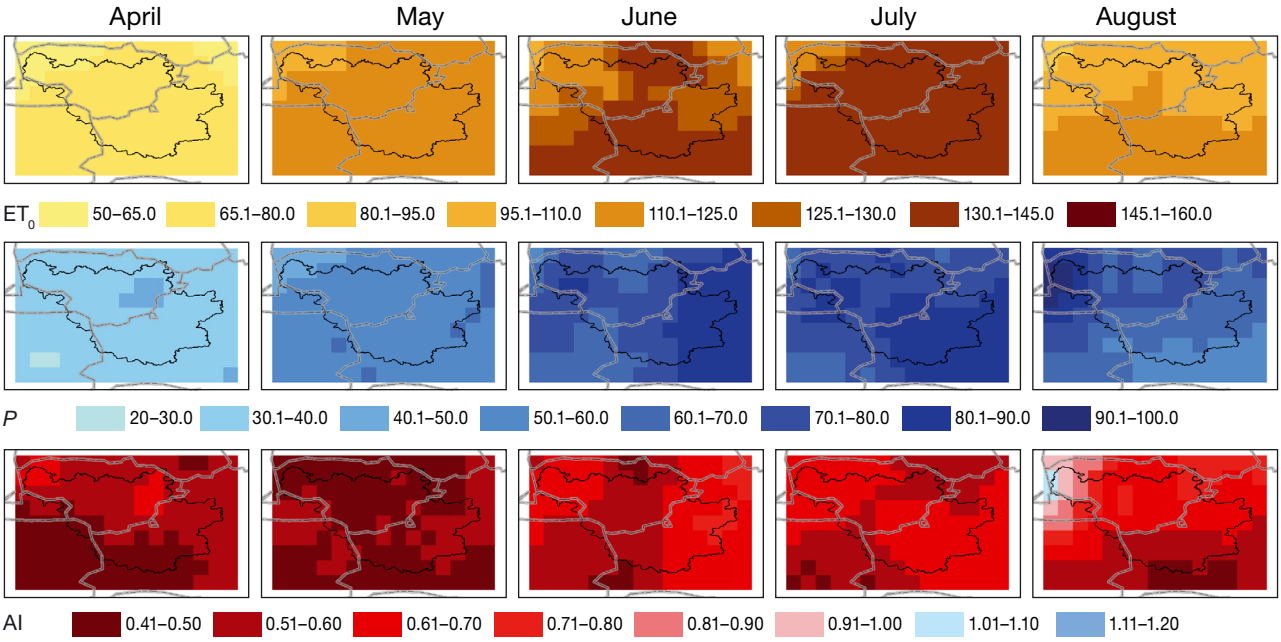

Fig. 3. Mean values of reference evapotranspiration (ET_0), precipitation amount (P) and aridity index (AI) in April–August 1981–2010. Black lines: Nemunas River Basin; grey lines: political boundaries

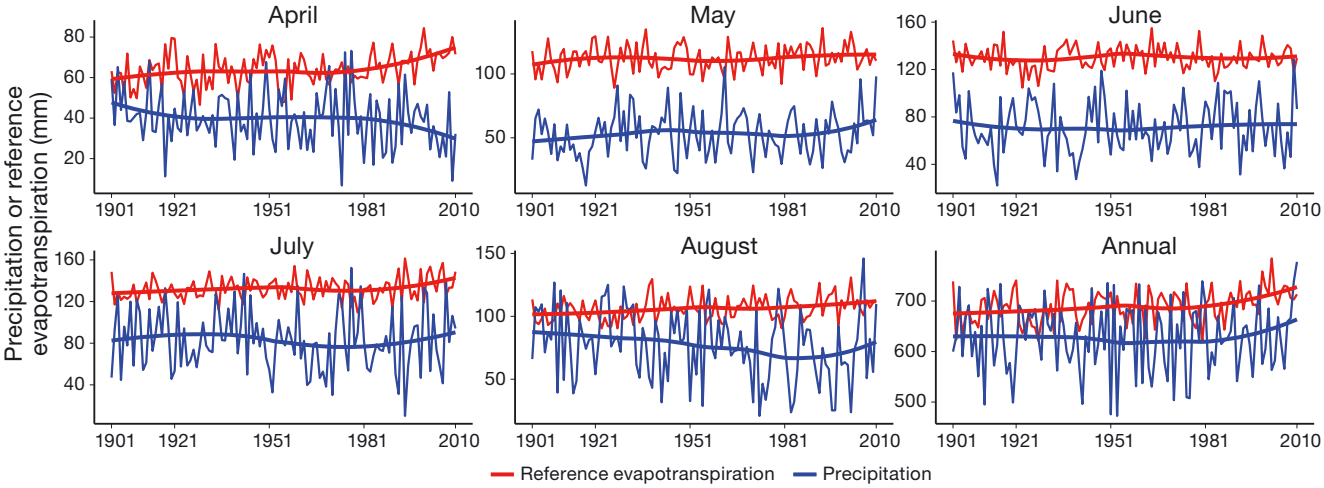

Fig. 4. Dynamics of the mean annual and monthly (April–August) precipitation and reference evapotranspiration in 1901–2010 in the investigation area

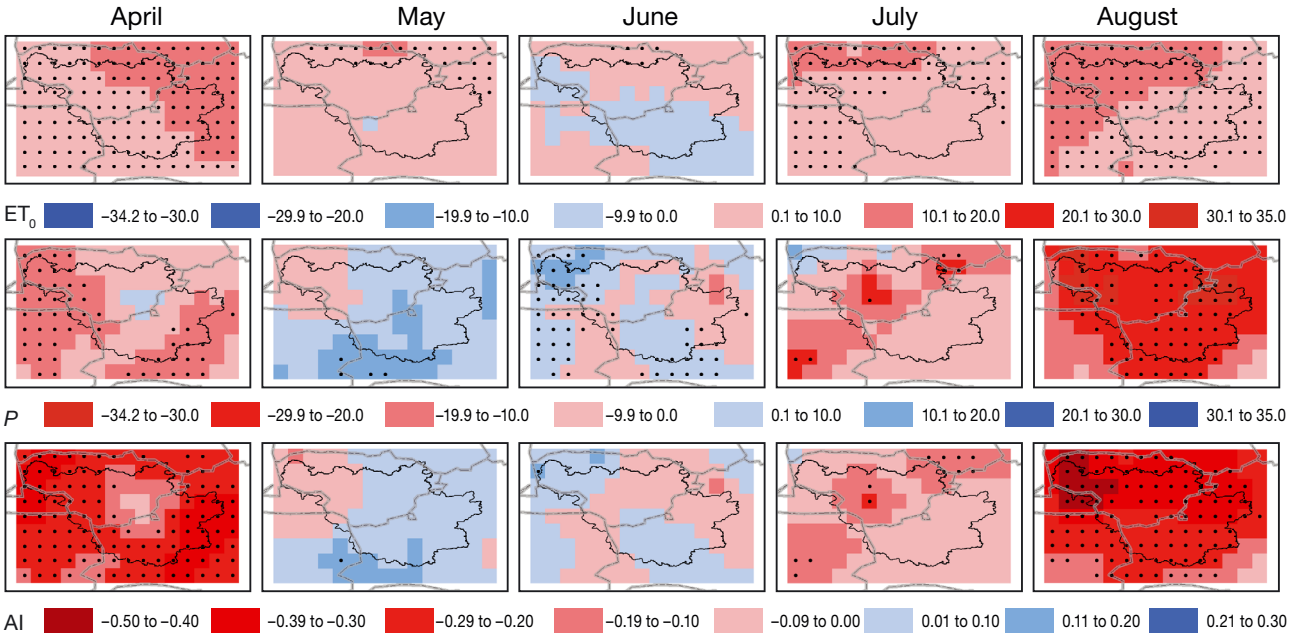

Fig. 5. Sen's slope trend values of reference evapotranspiration (ET_0), precipitation (P) and aridity index (AI) during 1901–2010. Black dots: cells with a statistically significant trend ($\alpha \leq 0.05$). Red colors: drying effect; blue colors: more humid climate. Black lines: Nemunas River Basin; grey lines: political boundaries

(Fig. 4) and the annual ET_0 exceeded P in 71% of the years. The standard deviation of the annual precipitation (SD = 67 mm) was more than twice as large as the variation in the ET_0 (SD = 32 mm). Annual ET_0 gradually increased during the whole period, with the steepest trend in recent decades. The amount of annual precipitation had no noticeable trend until the end of the 20th century; since the 1980s an increase in annual precipitation has been observed (Fig. 4).

Since the 1980s, a strong positive trend of ET_0 and a strong negative trend of P have been observed in April (Fig. 4). Such changes could be associated with weakening of westerlies in the second part of spring, because precipitation amounts in April are positively correlated with intensity of zonal circulation (Jaagus et al. 2010). During the whole period (1901–2010), the trend of ET_0 was statistically significant ($p \leq 0.05$) in all the grid cells, while the P trend was significant only in the western and southeastern parts of the Nemunas basin (Fig. 5). The resulting change in climate aridity was very sharp. The trend of the AI in April was significant in almost all the grid cells. In most of the domain the AI decreased by 0.20–0.40 throughout the analysed period. Even larger changes in aridity occurred in August. From the beginning of the 20th century up to the mid-1980s, August precipitation steadily decreased (Fig. 4). After the mid-1980s the decrease in precipitation slowed down and a small increase has been observed since the beginning of the 21st century (Fig. 4). The ET_0 in August had a stable and statistically significant positive trend during the entire 1901–2010 period. According to Sen's slope trend values, the ET_0 in August increased by 6–14 mm during 1901–2010, while P decreased by 20–35 mm. The climate aridity during August in the Nemunas basin has changed significantly due to changes in both ET_0 and P. The AI has decreased by 0.20–0.49. The largest changes occurred in the western part of the Nemunas basin (Fig. 5).

The changes in the ET_0 and P in May, June and July were smaller (Fig. 5). ET_0 had a small positive trend during 1901–2010 in May and July, while in June ET_0 increased in half the grid cells and decreased in the other half. The amount of precipitation during May and June increased in the majority of domain cells, but the trend was statistically significant only in the western and southeastern parts of the Nemunas basin in June (Fig. 5). The amount of precipitation decreased in July. The May–June patterns of the AI and P trends were similar and suggest that the changes in climate aridity during those months were related to the changes in precipitation. In July, the climate became drier, while May and June it became more humid in many parts of the Nemunas basin due to the increased precipitation.

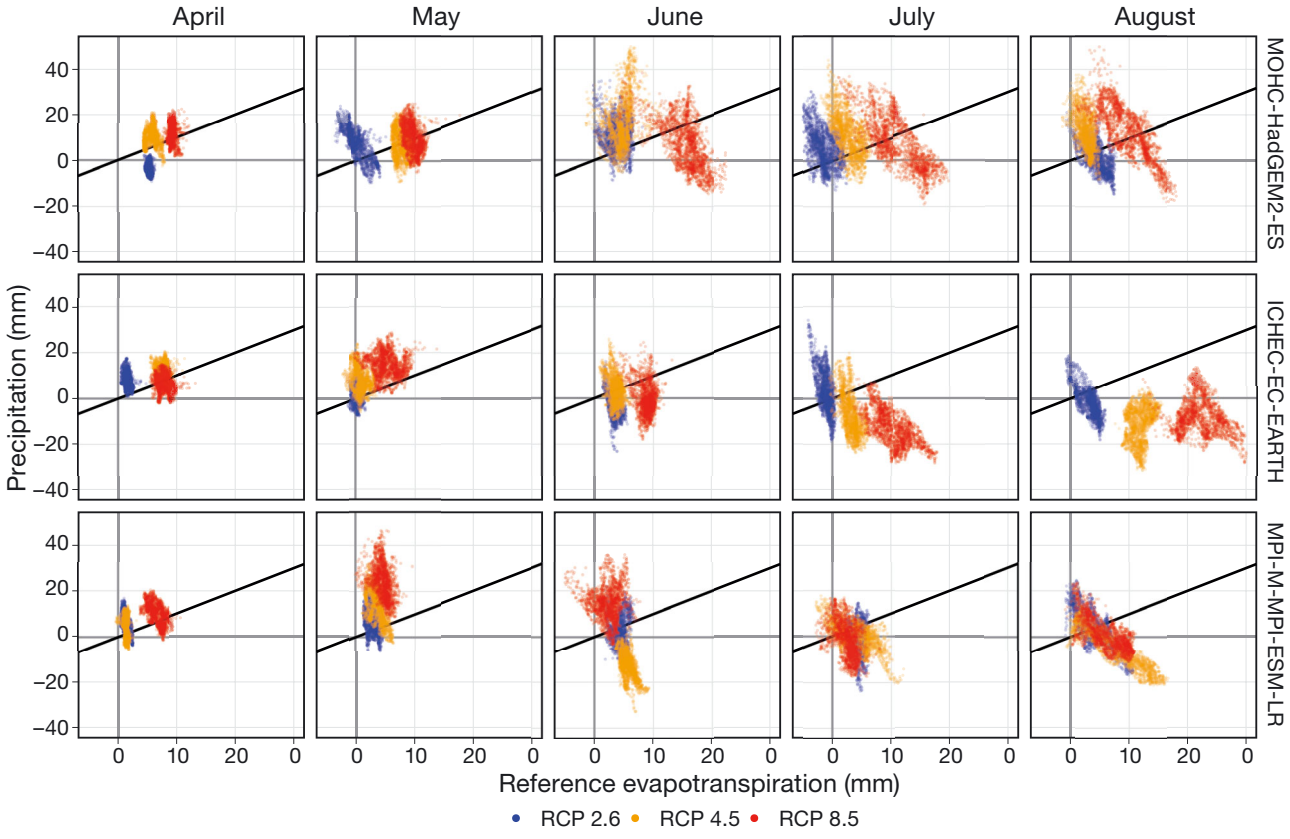

Fig. 6. Relationship between the projected changes in reference evapotranspiration and precipitation (difference between 2080–2099 and 1986–2005) in 2160 grid cells according to 3 RCP scenarios and 3 RCA4 simulations under different boundary conditions. Black reference line with slope = 1 indicates the precipitation values which compensate the changes in reference evapotranspiration. In the cells above the reference line the projected climate will be more humid; in the cells below the reference line the climate will be more arid

3.2 Projections of climate aridity

During the observation period the largest climate aridity changes were detected in April and August. There are large variations in the projected aridity changes up to the end of the 21st century (2080–2099) based on different simulations (Figs. 6 & 7). The projected precipitation changes according to a majority of the simulations and the RCP scenarios are larger than the changes in evapotranspiration (Fig. 6). In April, the variance in the projected *P* and ET_0 changes are smaller than in later months. It is likely that climate aridity will decrease slightly in April due to the increase in precipitation by up to 20 mm, and this increase will overcome the increase in ET_0 (Fig. 6). According to a majority of the projections, the climate in April is likely to become more humid in most of the domain (Fig. 7). The projections based on the MOHC-HadGEM2-ES model and RCP 2.6 scenario stand out. According to this scenario, the positive changes in ET_0 will be larger than those in *P*, and climate aridity will increase throughout the entire domain.

Precipitation is also likely to increase in May. According to most scenarios, ET_0 will also be higher, but the magnitude of the change will be less than the increase in precipitation, and the climate is likely to be more humid in most of the domain (Figs. 6 & 7).

Precipitation projections for June are more uncertain. June precipitation might increase according to some scenarios and simulations, but it might decrease according to others (Fig. 6). Possible changes in ET_0 are also uncertain. For example, according to the RCP8.5 scenario based on the MOHC-HadGEM2-ES simulation output, ET_0 might increase by 10–20 mm, while the projections based on the same scenario but on the MPI-M-MPI-ESM-LR simulation outputs suggest an increase in ET_0 of up to 7 mm in some cells and a decrease in others (Fig. 6).

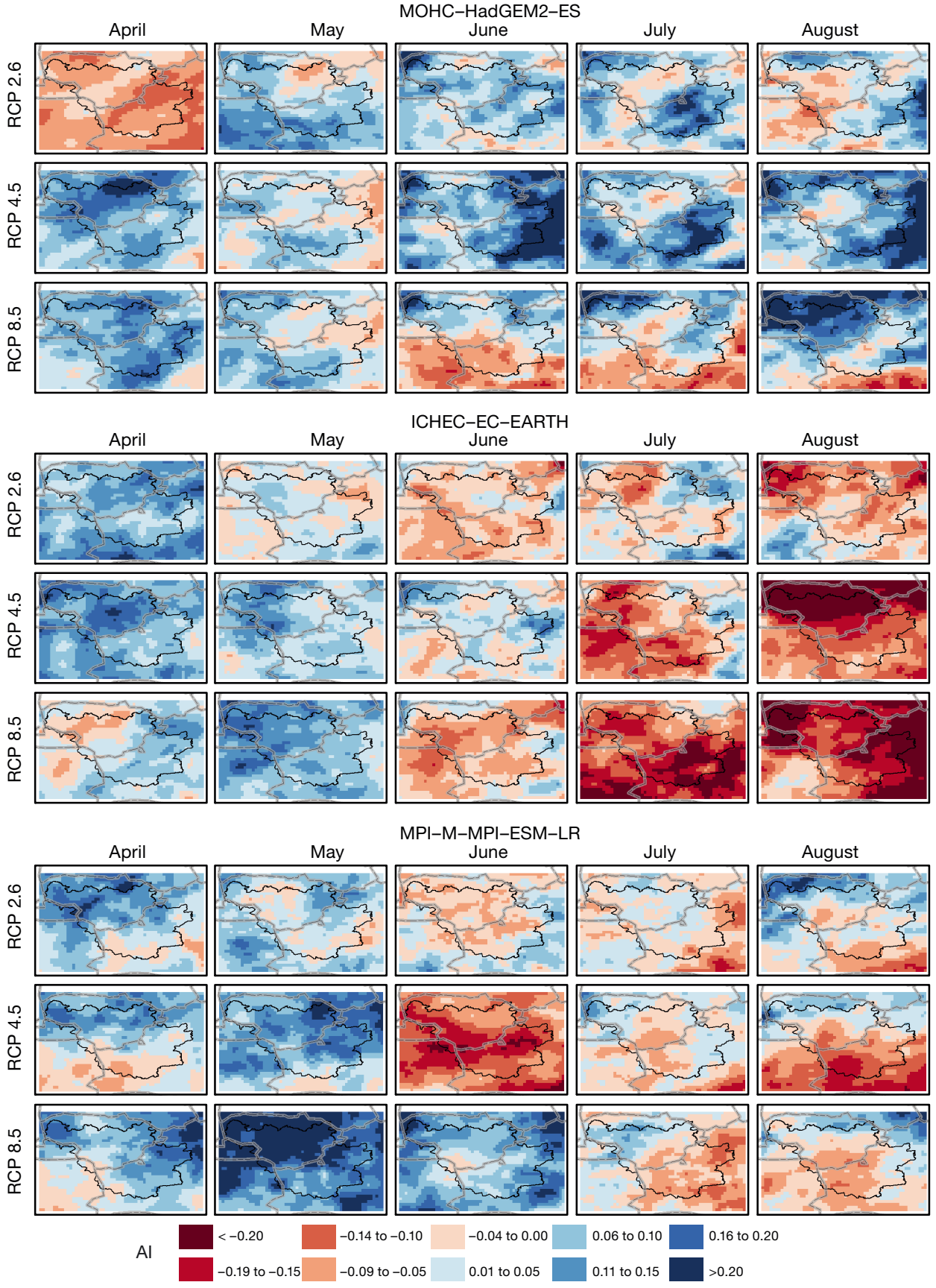

Fig. 7. Spatial pattern of the projected aridity index (AI) changes (difference between 1986–2005 and 2081–2100) in the analysed domain according to 3 simulations and 3 RCP scenarios. Blue colors: decrease in climate aridity; red colors: increase in aridity. Black lines: Nemunas River Basin; grey lines: political boundaries

The P and ET_0 projections for July based on the MOHC-HadGEM2-ES and ICHEC-EC-EARTH simulations are similar. According to both models, ET_0 is likely to decrease if climate change follows the RCP2.6 pathway, but it might increase if the climate changes according to the RCP4.5 and RCP8.5 scenarios.

The July precipitation projections based on the MOHC-HadGEM2-ES simulation indicate an increase in precipitation in most of the domain, while according to ICHEC-EC-EARTH, precipitation is likely to decrease. The uncertainty of the ET_0 projections inherited from the global circulation models used is the main reason why projections of changes in climate aridity are so different (Fig. 7). The July ET_0 and P projections based on the MPI-M-MPI-ESM-LR simulation output are very similar regardless of the RCP scenario. ET_0 is likely to increase by 0–10 mm in most of the domain, while P in some parts of the domain will increase by up to 20 mm and in others it will decrease by up to 20 mm.

According to the projections based on the M-MPI-ESM-LR model, changes in precipitation of the same magnitude as in July are likely in August. The ET_0 is likely to increase by 0–10 mm according to the RCP2.6 and RCP8.5 scenarios. The magnitude of this increase might be greater if climate change follows the RCP4.5 pathway. There is a close relationship between changes in the August P and the ET_0 projected using the M-MPI-ESM-LR model (Fig. 6). The greatest decrease in precipitation is projected for the cells with the greatest increase in ET_0. The spatial patterns of the projected changes in climate aridity based on the M-MPI-ESM-LR model are not very clear, but it is more likely that in the southern part of the domain the climate aridity may increase, while in the northern part it may decrease slightly. As in July, the biggest disparity is between the August P and ET_0 projections based on the MOHC-HadGEM2-ES and ICHEC-EC-EARTH models. According to ICHEC-EC-EARTH, the large increase in climate aridity in the domain is likely due to the increase in ET_0 and the decrease in P. The projections based on MOHC-HadGEM2-ES show that in most of the domain a precipitation increase is likely, the projected increase in ET_0 is smaller and climate aridity in most of the domain may decrease (Figs. 6 & 7).

Despite the large uncertainties in the climate projections, it is more likely that the Nemunas basin climate will become more humid in April–May and drier in June–August. An increase in climate aridity during these months is more likely in the southern and central parts of the basin.

4. DISCUSSION AND CONCLUSIONS

In a European context, EURO-CORDEX (Jacob et al. 2014) recently produced large ensembles of RCM simulations with approximately 12.5 and 50 km grid spacing, to which the RCA4 simulations contribute significantly. The RCM ensembles produced by EURO-CORDEX provide more detailed information (compared to GCM data) about future climate change scenarios (Kjellström et al. 2016). The regional scale projections give a more precise view of the climatic variables for medium-sized areas, although how the results are spread out is very much related to the choice of boundary conditions and model formulation (Figs. 6 & 7).

The previous version of RCA — the RCA3 model — tended to overestimate precipitation and surface evaporation over northern Europe during the summer season, whereas for most other regions and seasons the precipitation and surface turbulent fluxes were well simulated (Samuelsson et al. 2011). The analysis by Dieterich et al. (2013) covering the period 1970–1999 and by Wang et al. (2015) covering the period 1979–2010 showed that the RCA4-NEMO coupled model system is stable and suitable for different climate change studies.

Climate models show intensity-dependent biases which can alter the climate change signal (Boberg & Christensen 2012, Dosio 2016). The RCA4 projections for the Nemunas basin showed a huge variety of AI values (Figs. 6 & 7) depending on the GCM (MOHC-HadGEM2-ES, MPI-M-MPI-ESM-LR or ICHEC-EC-EARTH) simulations. The analysis of temperature and precipitation biases for the high-resolution EURO-CORDEX RCM by Dosio (2016) revealed that during the June–August (JJA) period all the RCMs driven by ICHEC-EC-EARTH showed a strong negative bias in every subregion, which implies a strong influence of the lateral boundary conditions on the RCM results. In our case, ICHEC-EC-EARTH gave the most dramatic changes in precipitation and AI values during JJA (Fig. 7). The large scatter in precipitation values for eastern Europe indicates a very small value of the original median climate signal (close to 0) and great intermodel variability (Dosio 2016).

The AI increased during the observation period (1901–2010) in the Nemunas basin during some months (April and August) of the dry period, whereas in other months the changes were insignificant. It can be concluded that the aridity of the investigated area increased slightly, especially in the last few decades. In the Nemunas basin the increase in arid-

ity was mostly related to the observed air temperature rise and consequently to the increase in ET_0, while decreased precipitation played a smaller role. Tabari & Aghajanloo (2013) also concluded that the increase in aridity was caused by the concurrent occurrences of positive ET_0 trends and negative *P* trends. Other studies show that AI values are most sensitive to changes in precipitation, and in regions with increasing precipitation this factor is more important than an air temperature rise (Huo et al. 2013).

Changes in *P* and ET_0 are likely to lead to more intense and possibly more frequent meteorological droughts in the Nemunas basin, and the meteorological conditions will have a significant effect on runoff there. The largest changes are more likely in the southern and eastern parts of the analysed area (Fig. 7). Drier conditions are also expected in southern parts of Europe (Nastos et al. 2013, Cheval et al. 2017). Meteorological and hydrological droughts frequently coincide at the end of the warm season (Rimkus et al. 2013). The projected decrease in the AI might lead to a reduction in runoff during the warm season low-flow period. The effect of increased aridity might be amplified by a reduction in the spring flood runoff volume, and the timing of spring flood may shift towards the beginning of the year. Changes in the spring flood runoff have been observed in the past (Stonevičius et al. 2014), and are very likely to occur in the future (Stonevičius et al. 2017). Shifts in the spring flood regime are likely to lead to a reduced base flow at the end of the 21st century. The projected increase in reference evapotranspiration and a smaller amount of precipitation at the end of summer are likely to reduce the amount of runoff formed during this period; consequently, the runoff from the Nemunas basin's rivers will be lower. Most sensitive to the projected changes might be river basins with large areas of open water. Evapotranspiration is limited by the amount of water on or near the surface, and is driven by atmospheric forcing. More intense forcing expressed as potential or reference evapotranspiration might not transform into evapotranspiration if the water is not available (Stonevičius et al. 2017). These tendencies are expected for most of the southern part of Europe, where actual evapotranspiration may decrease due to a significantly smaller amount of precipitation being available for evaporation (Cheval et al. 2017). The projected change in ET_0 and *P* might lead to lower water levels in lakes at the end of summer and the beginning of autumn. Most sensitive might be lakes with smaller catchment areas, because in these lakes precipitation and evaporation are more important in terms of total water balance.

A shift in the climate zone is probably a better measure of 'reality' for living systems, more so than changing temperature or precipitation (Gonzalez et al. 2010). Future changes in aridity patterns will lead to a change in the whole ecosystem mode, including aquatic (rivers, lakes, bogs and the Curonian lagoon) ones. The ecosystems are already shifting northwards, and this process will continue in the future (Rubel & Kottek 2010). The shifting of the winter and early spring runoff is very much influenced by snow climatology (Stonevičius et al. 2017), while in April–August it will be determined more by the ET_0 and *P* ratio.

Acknowledgements. This research is a part of a scientific study 'Impact assessment of climate change and other abiotic environmental factors on aquatic ecosystems' (project No. SIT-11/2015) funded under National Research Programme 'Sustainability of agro-, forest and water ecosystems (2015–2021)'.

LITERATURE CITED

Allen RG, Pereira LS, Raes D, Smith M (1998) Crop evapotranspiration: guidelines for computing crop requirements. Irrigation and Drainage Paper No. 56. FAO, Rome

Arora VK (2002) The use of the aridity index to assess climate change effect on annual runoff. J Hydrol (Amst) 265:164–177

BACC Author Team (2008) Regional climate studies: assessment of climate change for Baltic Sea region. Springer, Berlin

BACC II Author Team (2015) Regional climate studies: second assessment of climate change for the Baltic Sea basin. Springer International Publishing, Cham

Boberg F, Christensen JH (2012) Overestimation of Mediterranean summer temperature projections due to model deficiencies. Nat Clim Chang 2:433–436

Budyko MI (1958) The heat balance of the earth's surface. US Department of Commerce, Washington, DC

Cheval S, Dumitrescu A, Birsan MV (2017) Variability of the aridity in the south-eastern Europe over 1961–2050. Catena 151:74–86

Colantoni A, Ferrara C, Perini L, Salvati L (2015) Assessing trends in climate aridity and vulnerability to soil degradation in Italy. Ecol Indic 48:599–604

Collins WJ, Bellouin N, Doutriaux-Boucher M, Gedney N and others (2011) Development and evaluation of an earth-system model-HadGEM2. Geosci Model Dev 4: 1051–1075

De Martonne E (1926) Aréisme et indice artidite. C R Acad Sci Paris 182:1395–1398

Dieterich C, Schimanke S, Wang S, Väli G and others (2013) Evaluation of the SMHI coupled atmosphere-ice-ocean model RCA4_NEMO. Report Oceanography 47, Swedish Meteorological and Hydrological Institute, Norrköping

Dosio A (2016) Projections of climate change indices of temperature and precipitation from an ensemble of bias-

adjusted high-Resolution EURO-CORDEX regional climate models. J Geophys Res Atmos 121:5488–5511
Ficklin DL, Stewart IT, Maurer EP (2013) Climate change impacts on streamflow and subbasin-scale hydrology in the upper Colorado River Basin. PLOS ONE 8:e71297
Fniguire F, Laftouhi NE, Saidi ME, Markhi A (2014) Some aspects of climate variability and increasing aridity in central Morocco over the last forty years: case of Tensift Basin (Marrakech-Morocco). J Environ Earth Sci 4:42–51
Giorgetta MA, Jungclaus J, Reick CH, Legutke S and others (2013) Climate and carbon cycle changes from 1850 to 2100 in MPI-ESM simulations for the Coupled Model Intercomparison Project phase 5. J Adv Model Earth Syst 5:572–597
Girvetz EH, Zganjar C (2014) Dissecting indices of aridity for assessing the impacts of global climate change. Clim Change 126:469–483
Gonzalez P, Neilson RP, Lenihan JM, Drapek RJ (2010) Global patterns in the vulnerability of ecosystems to vegetation shifts due to climate change. Glob Ecol Biogeogr 19:755–768
Hargreaves GH (1994) Defining and using reference evapotranspiration. J Irrig Drain Eng 120:1132–1139
Hargreaves GH, Samani ZA (1985) Reference crop evapotranspiration from temperature. Appl Eng Agric 1:96–99
Harris IC, Jones PD (2017) CRU TS3.24: climatic research unit (CRU) time-series (TS) version 3.24 of high resolution gridded data of month-by-month variation in climate (Jan. 1901-Dec. 2015). Centre for Environmental Data Analysis, University of East Anglia Climatic Research Unit, Norwich
Hazeleger W, Severijns C, Semmler T, Ştefănescu S and others (2010) EC-Earth: a seamless earth-system prediction approach in action. Bull Am Meteorol Soc 91:1357–1363
Helsel DR, Hirsch RM (1992) Statistical methods in water resources. Studies in Environmental Science 49. Elsevier, New York, NY
Hordoir R, An BW, Haapala J, Dieterich C, Schimanke S, Höglund A, Meier HEM (2013) BaltiX: a 3D ocean modelling configuration for Baltic & North Sea exchange analysis. Report Oceanography 115, Swedish Meteorological and Hydrological Institute, Norrköping
Hrnjak I, Lukić T, Gavrilov MB, Marković SB, Unkašević M, Tošić I (2014) Aridity in Vojvodina, Serbia. Theor Appl Climatol 115:323–332
Huo ZL, Dai XQ, Feng SY, Kang SZ, Huang GH (2013) Effect of climate change on reference evapotranspiration and aridity index in arid region of China. J Hydrol (Amst) 492:24–34
IPCC (2013) Climate change 2013: the physical science basis. In: Stocker TF, Qin D, Plattner GK, Tignor M and others (eds) Contribution of Working Group I to the Fifth Assessment Report of the Intergovernmental Panel on Climate Change. Cambridge University Press, Cambridge
Jaagus J, Briede A, Rimkus E, Remm K (2010) Precipitation pattern in the Baltic countries under the influence of large-scale atmospheric circulation and local landscape factors. Int J Climatol 30:705–720
Jablonskis J (1992) Cyclic fluctuations of Lithuania rivers runoff. Energetika 4:16–37
Jacob D, Petersen J, Eggert B, Alias A and others (2014) EURO-CORDEX: new high resolution climate change projections for European impact research. Reg Environ Change 14:563–578
Jiménez Cisneros BE, Oki T, Arnell NW, Benito G and others (2014) Freshwater resources. In: Field CB, Barros VR, Dokken DJ, Mach KJ and others (eds) Climate change 2014: impacts, adaptation, and vulnerability. Part A: global and sectoral aspects. Contribution of Working Group II to the Fifth Assessment Report of the Intergovernmental Panel on Climate Change. Cambridge University Press, Cambridge, p 229–269
Kilkus K, Štaras A, Rimkus E, Valiuškevičius G (2006) Changes in water balance structure of Lithuanian rivers under different climate change scenarios. Environ Res Eng Manag 36:3–10
Kjellström E, Bärring L, Nikulin G, Nilsson C, Persson G, Strandberg G (2016) Production and use of regional climate model projections — a Swedish perspective on building climate services. Clim Serv 2-3:15–29
Klavins M, Briede A, Rodinov V, Kokorite I, Frisk T (2002) Long-term changes of the river runoff in Latvia. Boreal Environ Res 7:447–456
Korneev VN, Volchak AA, Hertman LN, Usava IP and others (2015) The strategic framework for adaptation to climate change in the Neman River basin. United Nations Development Programme, Belarus and United Nations Economic Commission for Europe, Brest
Kotlarski S, Keuler K, Christensen OB, Colette A and others (2014) Regional climate modeling on European scales: a joint standard evaluation of the EURO-CORDEX RCM ensemble. Geosci Model Dev 7:1297–1333
Kriaučiūnienė J, Meilutytė-Barauskienė D, Rimkus E, Kažys J, Vincevičius A (2008) Climate change impact on hydrological processes in Lithuanian Nemunas river basin. Baltica 21:51–61
Kriauciuniene J, Meilutyte-Barauskiene D, Reihan A, Koltsova T, Lizuma L, Sarauskiene D (2012) Variability in temperature, precipitation and river discharge in the Baltic states. Boreal Environ Res 17:150–162
Kukal M, Irmak S (2016) Long-term patterns of air temperatures, daily temperature range, precipitation, grass-reference evapotranspiration and aridity index in the USA Great Plains. II. Temporal trends. J Hydrol (Amst) 542: 978–1001
Kundzewicz ZW, Mata LJ, Arnell NW, Döll P and others (2007) Freshwater resources and their management. In: Parry M, Canziani O, Palutikof J, van der Linden P (eds) Climate change 2007: impacts, adaptation and vulnerability. Contribution of Working Group II to the Fourth Assessment Report of the Intergovernmental Panel on Climate Change. Cambridge University Press, Cambridge, p 173–210
Kupiainen M, Jansson C, Samuelsson P, Jones C and others (2014) Rossby Centre regional atmospheric model, RCA4. Swedish Meteorological and Hydrological Institute, Norrköping https://www.smhi.se/en/research/research-departments/climate-research-rossby-centre2-552/rossby-centre-regional-atmospheric-model-rca4-1.16562
Li B, Chen F (2015) Using the aridity index to assess recent climate change: a case study of the Lancang River Basin, China. Stochastic Environ Res Risk Assess 29:1071–1083
Maliva R, Missimer T (2012) Aridity and drought. In: Arid lands water evaluation and management. Environmental Sciences and Engineering (Environmental Engineering), Springer-Verlag, Berlin, p 21–39
McKee TB, Doesken NJ, Kleist J (1993) The relationship of drought frequency and duration to time scales. In: Proc 8th Conf Applied Climatology, Anaheim, CA, 17–22 Jan 1993. American Meteorological Society, Washington,

DC, p 179–184
Meilutytė-Barauskienė D, Kovalenkovienė M, Irbinskas V (2008) Water resources of Lithuanian rivers and their relation to climate change. Geografija 44:1–8 (in Lithuanian)
Middleton NJ, Thomas DSG (1997) World atlas of desertification, 2nd edn. UNEP, Edward Arnold, London
Millennium Ecosystem Assessment (2005) Living beyond our means: natural assets and human well-being. Statement from the board. United Nations Environment Programme, Geneva
Naiman RJ, Dêcamps H, McClain ME (2005) Riparia: ecology, conservation and management of streamside communities. Elsevier, Amsterdam
Nalbantis I, Tsakiris G (2009) Assessment of hydrological drought revisited. Water Resour Manage 23:881–897
Nastos PT, Politi N, Kapsomenakis J (2013) Spatial and temporal variability of the aridity index in Greece. Atmos Res 119:140–152
Palmer WC (1965) Meteorological drought. Res Pap No. 45, US Weather Bureau, Washington, DC
Paltineanu C, Mihailescu IF, Seceleanu I, Dragota C, Vasenciuc F (2007) Using aridity indices to describe some climate and soil features in eastern Europe: a Romanian case study. Theor Appl Climatol 90:263–274
Paulo AA, Rosa RD, Pereira LS (2012) Climate trends and behaviour of drought indices based on precipitation and evapotranspiration in Portugal. Nat Hazards Earth Syst Sci 12:1481–1491
Penman HL (1948) Natural evaporation from open water, bare soil and grass. Proc R Soc Lond A Math Phys Sci 193:120–145
Rimkus E, Stonevičius E, Korneev V, Kažys J, Valiuškevičius G, Pakhomau A (2013) Dynamics of meteorological and hydrological droughts in the Neman river basin. Environ Res Lett 8:045014
Rivas-Martinez S, Rivas-Saenz S, Penas A (2011) Worldwide bioclimatic classification system. Global Geobotany 1: 1–634
Rubel F, Kottek M (2010) Observed and projected climate shifts 1901–2100 depicted by world maps of the Köppen-Geiger climate classification. Meteorol Z (Berl) 19: 135–141
Sailer B (2013) Climate change scenarios in international river basins: Is the uneven distribution of water resources increasing? MSc thesis, University of Freiburg
Samuelsson P, Jones C, Willen U, Ullerstig A and others (2011) The Rossby Centre regional climate model RCAS3: model description and performance. Tellus, Ser A, Dyn Meterol Oceanogr 63:4–23
Sarauskiene D, Kriauciuniene J, Reihan A, Klavins M (2015) Flood pattern changes in the rivers of the Baltic countries. J Environ Eng Landsc 23:28–38
Selianinov GT (1928) On agricultural climate valuation. Proc Agric Meteor 20:165–177
Stahl K, Tallaksen LM, Hannaford J, van Lanen HAJ (2012) Filling the white space on maps of European runoff trends: estimates from a multi-model ensemble. Hydrol Earth Syst Sci 16:2035–2047
Stonevičius E, Valiuškevičius G, Rimkus E, Kažys J (2014) Climate induced changes of Lithuanian rivers runoff in 1960–2009. Water Resour 41:592–603
Stonevičius E, Rimkus E, Štaras A, Kažys J, Valiuškevičius G (2017) Climate change impact on the Nemunas River basin hydrology in the 21st century. Boreal Environ Res 22:49–65
Strandberg G, Bärring L, Hansson U, Jansson C and others (2014) CORDEX scenarios for Europe from the Rossby Centre regional climate model RCA4. Report Meteorology and Climatology 116, Swedish Meteorological and Hydrological Institute, Norrköping
Tabari H, Aghajanloo MB (2013) Temporal pattern of aridity index in Iran with considering precipitation and evapotranspiration trends. Int J Climatol 33:396–409
Taylor KE, Stouffer RJ, Meehl GA (2012) An Overview of CMIP5 and the experiment design. Bull Am Meteorol Soc 93:485–498
ter Heerdt GN, Schep SA, Janse JH, Ouboter M (2007) Climate change and the EU Water Framework Directive: How to deal with indirect effects of changes in hydrology on water quality and ecology? Water Sci Technol 56:19–26
Thornthwaite CW (1948) An approach toward a rational classification of climate. Geogr Rev 38:55–94
UNESCO (1979) Map of the world distribution of arid regions: explanatory note. MAB technical notes 7. UNESCO, Paris
Volchak A (2004) Calculation and forecast of the annual discharge of the Neman River in Byelorussia. Int BALTEX Secretariat Publ 29:141–142
Wang S, Dieterich C, Döscher R, Höglund A and others (2015) Development and evaluation of a new regional coupled atmosphere ocean model in the North Sea and Baltic Sea. Tellus, Ser A, Dyn Meterol Oceanogr 67:24284
Wilson D, Hisdal H, Lawrence D (2010) Has streamflow changed in the Nordic countries? Recent trends and comparisons to hydrological projections. J Hydrol (Amst) 394:334–346
Zhang Q, Xu CY, Zhang Z (2009) Observed changes of drought/wetness episodes in the Pearl River basin, China, using the standardized precipitation index and aridity index. Theor Appl Climatol 98:89–99

Editorial responsibility: Filippo Giorgi, Trieste, Italy/ Mikhail Semenov, Harpenden, UK

Submitted: November 15, 2017; Accepted: March 14, 2018
Proofs received from author(s): May 26, 2018